plane and results in many (or one) reentrant corners at the needle tip (Fig. 9b). The easy nucleation at the reentrant sites leads to a sharp appearance on the top of crystal and will further result in the needle growth.

In general, the dendritic crystal will occur on the condition of low MTS concentration, whose supersaturation is too high for whisker growth. The dendrites grow perpendicularly from the substrate surface. It has a yellow translucent (for pure β-SiC) or dark gray (with impurity) appearance and a very pronounced ribbed structure with well-developed stalk and branching arms (Fig. 10). From the observation of the growth features, the TPRE mechanism which is responsible for dendritic growth (22) is evident.

Conclusion

The deposition of silicon carbide from methyltrichlorosilane by the low pressure chemical vapor deposition was studied. The rate of deposition depends on the deposition temperature and MTS flux. At higher temperatues the growth rate of films is affected by both the mass-transfer diffusion limit and thermal etching. At lower temperatures, the growth rate is primarily controlled by surface kinetics. The growth texture of β-SiC films is dependent on the deposition time and growth rate. However, the major preferred orientation is (220). The propagation of films is attributed to the twin plane reentrant edge mechanism, which is also responsible for the growth of particulate crystals.

Manuscript submitted Feb. 12, 1987; revised manuscript received June 24, 1987.

National Cheng Kung University assisted in meeting the publication costs of this article.

REFERENCES

1. J. W. Faust, Jr., in "Silicon Carbide—1973," R. C. Marshall, J. W. Faust, Jr., and C. E. Ryan, Editors, p. 668, University of South Carolina Press, Columbia, SC (1974).
2. D. P. Stinton and W. J. Lackey, *Ceram. Bull.*, **57,** 568 (1978).
3. H. G. Lipon, in "Silicon Carbide—A High Temperature Semiconductor," J. R. O'Connor and J. Smiltens, Editors, p. 371, Pergamon Press, Oxford (1960).
4. J. Schlichting, *Powder Metall. Int.*, **12,** 141 (1980); continued **12,** 196 (1980).
5. J. R. Weiss and R. J. Diefendorf, in "Silicon Carbide—1973," R. C. Marshall, J. W. Faust, Jr., and C. E. Ryan, Editors, p. 80, University of South Carolina Press, Columbia, SC (1974).
6. W. F. Knippenberg, G. Verspui, and A. W. C. von Kemenade, in "Silicon Carbide—1973," R. C. Marshall, J. W. Faust, Jr., and C. E. Ryan, Editors, p. 92, University of South Carolina Press, Columbia, SC (1974).
7. J. Chin, D. K. Gantzel, and R. G. Hudson, *Thin Solid Films*, **40,** 57 (1977).
8. S. S. Shinozaki and H. Sato, *J. Am. Ceram. Soc.*, **61,** 425 (1978).
9. E. Sirtl, L. P. Hunt, and H. Sawyerl, *This Journal*, **121,** 919 (1974).
10. J. M. Harris, *ibid.*, **118,** 335 (1971).
11. A. W. C. von Kemenade and C. F. Stemfoort, *J. Cryst. Growth*, **12,** 13 (1972).
12. J. I. Federer, *Thin Solid Films*, **40,** 89 (1977).
13. C. H. J. von den Brekel, *Philips Res. Rep.*, **32,** 118 (1977).
14. T. D. Gulden, *J. Am. Ceram. Soc.*, **51,** 424 (1968).
15. R. S. Wagner, *Acta Metall.*, **8,** 57 (1960).
16. D. R. Hamilton and R. G. Seidensticker, *J. Appl. Phys.*, **31,** 1165 (1960).
17. J. W. Faust, Jr. and H. F. John, *J. Phys. Chem. Solids*, **25,** 1407 (1964).
18. W. Berriman and R. H. Herz, *Nature*, **180,** 239 (1957).
19. J. W. Matthews and D. L. Allinson, *Philos. Mag.*, **8,** 1283 (1963).
20. S. Mendelson, *J. Appl. Phys.*, **36,** 2525 (1965).
21. J. F. Hamilton and L. E. Brady, *ibid.*, **35,** 414 (1964).
22. D. J. Cheng, W. J. Shyy, and M. H. Hon, *Scri. Metall.*, **20,** 1587 (1986).

Selective Area Growth of High Quality GaAs by OMCVD Using Native Oxide Masks

Stephen H. Jones* and Kei May Lau**

Department of Electrical and Computer Engineering, University of Massachusetts, Amherst, Massachusetts 01003

ABSTRACT

A study of selective area growth by atmospheric pressure organometallic chemical vapor deposition (OMCVD) using plasma-grown GaAs native oxide masks was conducted. Deposition experiments were carried out with different growth parameters to observe the variation of polycrystalline coverage on the oxide mask. With high growth temperatures or low V/III ratios, poly deposition on the mask was depleted, particularly in regions near the unmasked single-crystal areas. With the optimum conditions for GaAs growth, the polycrystalline growth was homogeneous to the single-crystal boundary, and the single-crystal GaAs areas exhibited liquid nitrogen mobilities up to 105,000 cm^2/Vs. Etch-and-fill experiments were also performed using a NH_4OH based etch to obtain near vertically etched sidewalls. Growth from the walls caused little distortion at the edges of the filled pockets and flat single-crystal surfaces were obtained.

As chloride vapor phase epitaxy and liquid phase epitaxy became viable technologies for compound semiconductors, selective epitaxial growth was proposed and explored (1, 2). Etch-and-fill experiments using SiO_2 as a dielectric mask were performed, and, as expected, single crystal GaAs grew in the exposed areas of the substrate and no growth was observed on the mask. However, severe corner facet formation forced the selective growth within the rectangular and circular mask openings into distorted polygonal mesa structures (3, 4). This distortion of the surface geometry precluded many practical applications of selective epitaxy. In recent years the increasing demands for GaAs-based integrated circuits using organometallic chemical vapor deposition (OMCVD) and molecular beam epitaxy (MBE) technologies have generated renewed interest in selective area epitaxy. Furthermore, the emergence of new devices such as the permeable base transistor has triggered intensive efforts to develop lateral overgrowth techniques on tungsten gratings (5, 6). In addition to the most commonly used SiO_2 mask, other dielectrics such as SiN_x, AlN, and shadow masks have been used for patterning the growth (7-9). Although GaAs native oxide masks have been utilized with MBE (10, 11), applying native oxide masks to the higher temperature selective OMCVD process has not been previously studied.

For some device applications, deposition of polycrystalline materials is undesirable and efforts have been made to prevent nucleation on the masks (12). However, since polycrystalline GaAs (poly-GaAs) is highly resistive, it could be used for isolation and bridging in integrated circuits (13). In addition, because of its high resis-

* Electrochemical Society Student Member.
** Electrochemical Society Active Member.

tivity, light sensitivity, and presumably very short carrier recombination times (14, 15), poly-GaAs is a candidate for ultrafast photoconductor material.

In this paper, we report a thorough study concerning selective area deposition on native oxide patterned GaAs substrates using OMCVD. The growth characteristics and material properties of both the single-crystal GaAs in isolated areas the the poly-GaAs on the oxide were investigated.

Experiments

Patterning process.—The photo mask used for the selective epitaxy experiments includes lines, patches, and square rings with various dimensions and spacings (Fig. 1). In addition to studying the effects of crystal orientation on the single-crystal and polycrystalline growth, the characteristics of the poly/single-crystal interface can also be observed for different surface geometries. There are large 3 × 3 mm patches for electrical measurements such as Hall mobilities and C-V profiling, while the smaller 10-400 μm geometries are for SEM and optical microscope characterization.

The native oxides were generated on (100) misoriented 2° towards (110) substrates using the plasma oxidation technique (16, 17). For our native oxide growth, a Technic PE-IIA/PD-IIA parallel plate plasma etch/deposition system was used, and the range of parameters were: oxygen pressures between 200 and 350 μm, substrate temperature from 200° to 350°C, RF powers between 200 and 400W, and oxidation times from 10 to 30 min. The resulting oxide layers, thought to be amorphous $GaAsO_3$ (16), were typically 150-250Å thick, as determined by ellipsometry.

After oxidation, the wafers were immediately patterned using a conventional positive photoresist procedure. Once patterned, the oxide was selectively removed using a 1:10 ($HF:H_2O$) etch followed by a 1:10 ($H_2O_2:H_2O$) dip and DI water rinse (10). The HF readily removes the oxide, while the H_2SO_4 based etch does not attack the oxide layer. In order to improve the surface quality of the opened areas in the oxide, a subsequent 1:1:150 ($H_2SO_4:H_2O_2H_2O$) 5s etch was performed following the oxide removal.

For etch-and-fill experiments, 3-4 μm of the substrate was etched after the oxide pattern had been generated. Two etching systems with different etching profiles were used to investigate the selective growth within the 3-4 μm recessed patterns: the H_2SO_4 acid system and the NH_4OH base system. Initially, a 1:1:8 ($H_2SO_4:H_2O_2:H_2O$) system was chosen since it etches smooth, flat-bottomed holes at approximately 0.2 μm/min (18). However, the cleaved cross section of etched samples revealed nonvertical sidewalls. Since the intention of the selective growth was to fill in the holes and grooves with minimal distortion at the walls, the nonvertical sidewalls from the H_2SO_4 system were undesirable. Therefore a 1:1:10 ($NH_4OH:H_2O_2:H_2O$) etch system which generates nearly vertical sidewalls traveling in the [011] direction was used for most of the experiments. Although this base etch does create more ideal sidewalls in the [011] direction, it does not create as flat a hole bottom as the H_2SO_4 etch.

Selective growth.—The experiments were performed with an in-house built, computer-controlled OMCVD system. The horizontal reaction chamber configuration consisted of a 13 in. long 50 mm ID tube, with a centered 4 × 6 cm SiC coated graphite susceptor. The growth parameters studied were: temperatures from 600° to 750°C, V/III ratios between 4 and 60, total flows of 5 l/min, and trimethylgallium (TMG) mole fractions of 2-4 × 10^{-4}. All experiments were carried out at atmospheric pressure. To better reveal the nature of the selective area growth, 500Å heavily doped marker layers were placed between each of six 5000Å undoped layers. By cleaving and staining the layers, the lateral and other nonvertical growth could be examined. For electrical measurements on the 3 × 3 mm patches, several 5-9 μm undoped single layers were grown.

Discussion and Results

Dependence of polycrystalline GaAs coverage on growth parameters and mask geometry.—For the $GaAsO_3$ surface, there are characteristic temperatures at which the reactants [Ga, $Ga(CH_3)_3$, $GaCH_3$, AsH_3, AsH, etc.] begin to surface migrate. If the growth is carried out below the required temperature for this to occur significantly, the poly-GaAs will grow uniformly to the single-crystal boundary. However, at higher temperatures when surface diffusion becomes important, the operating pressure, temperature, and reactant partial pressures will greatly influence the diffusion coefficient (19, 20). By increasing the diffusion coefficient and therefore the diffusion length at reduced pressures and/or elevated temperatures the reactant species can migrate extensively over the $GaAsO_3$ surface, the result being a net migration to the unmasked single-crystal surfaces where the reaction efficiency is higher due to increased sticking coefficient, reduced activation energies, or lower surface

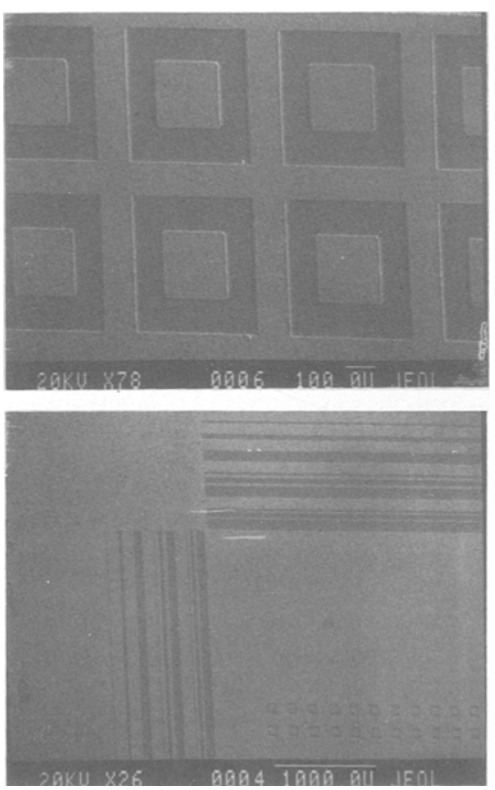

Fig. 1. (a, top) Large single-crystal GaAs square rings surrounded by homogeneous poly-GaAs. (b, bottom) [011] and [011] directed line sets of single-crystal GaAs among poly-GaAs. Smallest line width of 10 μm. Also shown are small square GaAs rings. Growth temperature = 700°C, AsH_3/TMG = 45.

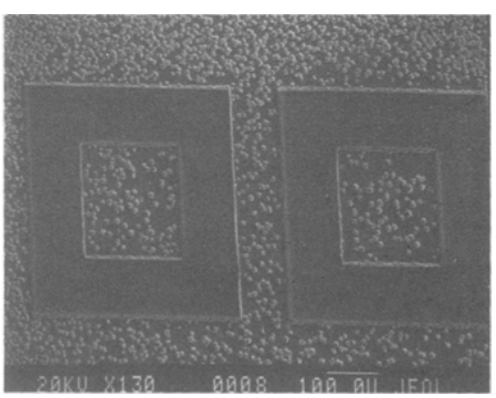

Fig. 2. Large single-crystal GaAs square rings surrounded by sparse poly-GaAs deposition. Growth temperature = 750°C, AsH_3/TMG = 45.

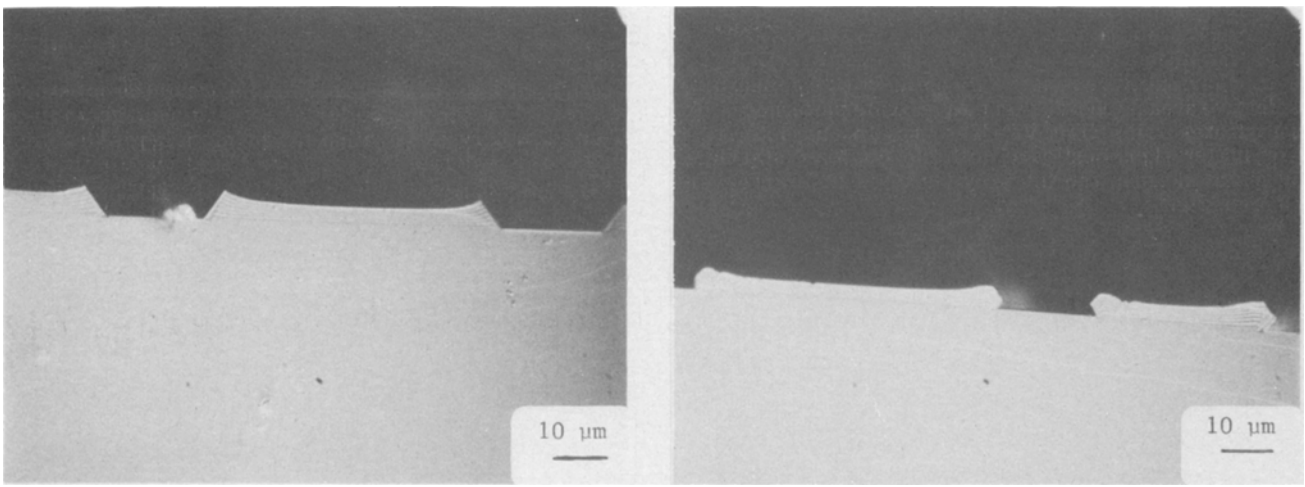

Fig. 3. Reduced poly-GaAs nucleation on the native oxide mask and enhanced single-crystal growth at the mask/single crystal interface. (a, left) Cross-sectional view, cleaved along the (011) plane; (b, right) cross-sectional view, cleaved along the (0$\bar{1}$1) plane. Growth temperature = 750°C, AsH_3/TMG = 45.

potentials (21, 22). Consequently, within some diffusion length from the mask/single-crystal interface, there can be minimal nucleation on the mask and growth enhancement in the single-crystal region.

In a set of experiments we performed at various temperatures (P = 1 atm), we observed that the poly-GaAs growth was homogeneous to the single crystal boundary at 700°C or below (Fig. 1). However, at 750°C, we found the poly-GaAs deposition on the oxide sparse and even depleted in some areas (Fig. 2). The extent of poly-GaAs coverage on the oxide was found to be dependent on the mask geometry. The poly-GaAs was always found to be uniform and dense far away from any single-crystal regions (> 100 μm) for all growth temperatures between 600°-750°C. Yet, for small mask linewidths (≲ 25 μm) between larger single-crystal linewidths (≳ 25 μm), the poly-GaAs deposition was depleted in the 700°-750°C temperature range. The mask linewidths necessary to assure no poly-GaAs growth within a given substructure may vary from one to tens of microns depending on the growth temperature. As the temperature is increased above 700°C nucleation on 15-20 μm linewidth oxides significantly decreases. Meanwhile, as the poly-GaAs was depleted within the substructures, enhancement of single-crystal growth occurred at the mask/single-crystal interface. The degree of enhancement was again dependent on the oxide linewidth and the growth parameters (Fig. 3). The migration of the gallium constituents from the oxide to the GaAs during growth seems to explain these results.

However, the amount of growth rate enhancement in the single-crystal regions does not account for all of the undeposited poly which did not nucleate on the oxide. It is believed that in conjunction with surface migration, a considerable amount of reactants may diffuse back to the gas stream. From Fig. 3a, the approximate percent contribution to the total single-crystal growth rate from the vacant oxide regions can be estimated. Based on calibrated growth rates, the anticipated thickness at the center of the mesa should be 3 μm without contributions from surface migration. A rough calculation of the growth enhancement showed that only an estimated 30-40% of the material from the oxide regions contributed to the total thickness of the single-crystal mesa. Although this figure is a gross estimate, it qualitatively emphasizes that not only surface migration is prevalent, but that diffusion back to the gas stream readily occurs. At either high temperature or low pressure, diffusion could be so free that growth on all the masked regions will not occur. Researchers using SiO_2, AlN, SiN_x, and tungsten as a masking material have reported similar variations in the homogeneity of the poly/single-crystal interface with different growth parameters. Complete absence of poly growth using low pressure and SiN_x masks has been obtained (12); while homogeneous coverage up to the single-crystal boundary with AlN masks (8) has also been observed. Based on the previous and current results, we believe that independent of the mask used, one can find a set of growth parameters to control the nucleation on the mask within some substructure. Our results indicate that if native oxide masks at atmospheric pressure and 750°C are utilized, then oxide substructures at 15-20 μm or less linewidth will be free of polycrystalline deposition.

The extent of poly coverage as a function of AsH_3/TMG ratio was also investigated. It was found that at low AsH_3/TMG ratios ($X_{AsH_3} = 8 \times 10^{-4}$, $X_{TMG} = 2 \times 10^{-4}$) the poly coverage becomes sparse in the vicinity of single-crystal regions (Fig. 4 and 5). We are not certain which effect, the low ratio or low arsine mole fraction, dominates the lack of nucleation on the oxide. However, it is apparent that the arsine plays an important role in the diffusion and nucleation process on the mask. It should be noted that such low ratios will not produce high quality GaAs with our reactor configuration.

Orientation dependence of selective single-crystal growth.—As with the polycrystalline growth, we found that the characteristics of the selective growth in the single-crystal regions are strongly influenced by the diffusion of the Ga-bearing species at the solid surface. However, since the growth in the single-crystal regions is epitaxial and not disordered poly-GaAs deposition, the crystal orientation dominates the properties of the single-crystal GaAs at the oxide/GaAs interface. Although the extent of diffusion from the mask region may differ depending on the mask material (SiO_2, SiN_x, Ga_2O_3, $GaAsO_3$), the characteristics of the GaAs at the interface are predetermined by the crystal orientation and

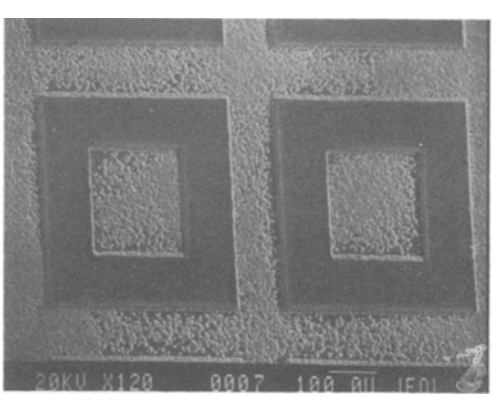

Fig. 4. Large single-crystal GaAs square rings surrounded by sparse poly-GaAs deposition. Growth temperature = 700°C; AsH_3/TMG = 4; $X_{AsH_3} = 8 \times 10^{-4}$.

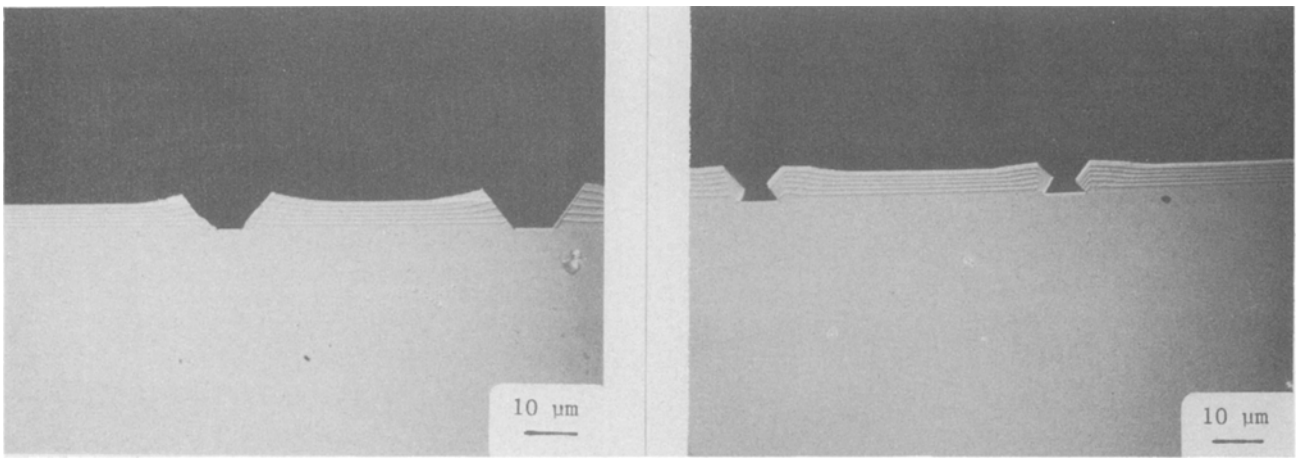

Fig. 5. Reduced poly-GaAs nucleation on the native oxide mask between single crystal GaAs lines. (a, left) Cross-sectional view, cleaved along the (011) plane; (b, right) cross-sectional view, cleaved along the (0$\bar{1}$1) plane. Growth temperature = 700°C; $AsH_3/TMG = 4$; $X_{AsH_3} = 8 \times 10^{-4}$.

are independent of the mask. For instance, single-crystal lines traveling in a particular direction have the same growth characteristics at the boundary whether the boundary is native oxide or a single-crystal mesa (Fig. 6 and 7). For lines traveling in the [011] and [0$\bar{1}$1] directions, the interface will always reveal the (111)A slow growth planes (Fig. 8) (22). This can be explained by surface migration, and inhibited growth on the (111)A planes. A Ga-species surface attachment scheme proposed by Reep and Ghandi to explain extensive faceted growth on (111)A oriented substrates reflects the nature of the selectively grown interface (23).

Depending on the atomic arrangement at the crystal surface, the various crystal faces can be categorized into flat, stepped, or kinked surfaces (24). The (100) plane is a combination of stepped and kinked, while the |111| planes are flat. Due to the surface atomic structure, the desorption of the methyl(s) group from the growth surface of the (111)A plane is thought to inhibit the growth under mass transfer conditions (23). For the selective

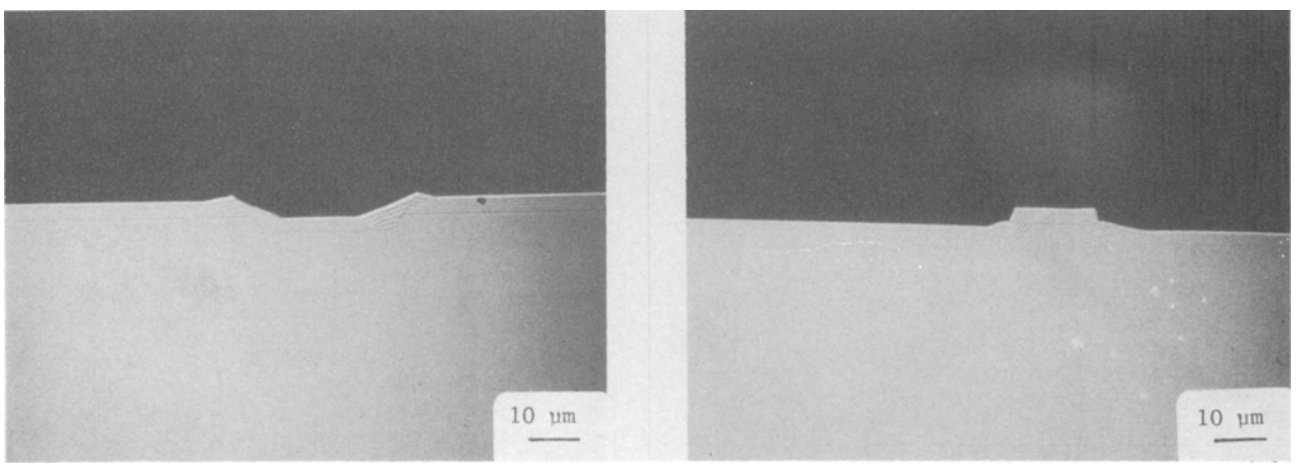

Fig. 6. Emergence of the |111|A low growth-rate planes for regrown GaAs. Etchant used was 1:1:8:H_2SO_4:H_2O_2:H_2O. (a, left) Cross-sectional view, cleaved along the (011) plane of growth in and around a [011] directed trough; (b, right) same sample cleaved along the (0$\bar{1}$1) plane of a [0$\bar{1}$1] directed trough. Growth temperature = 700°C; $AsH_3/TMG = 45$.

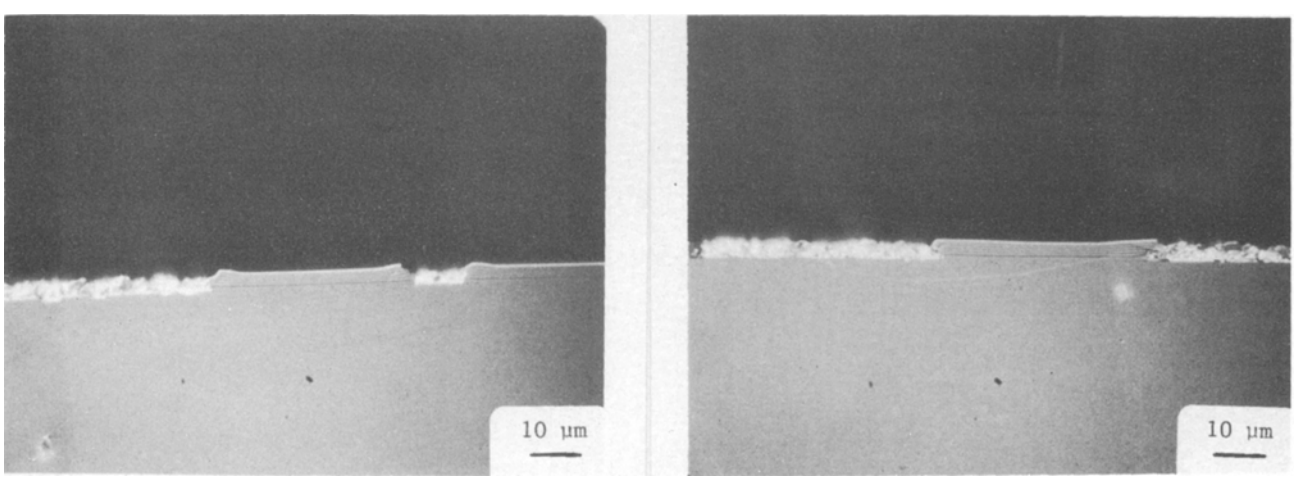

Fig. 7. Emergence of the |111|A low-growth-rate planes for selectively grown GaAs. Homogeneous poly-GaAs separating (a, left) [011] directed single-crystal GaAs lines; (b, right) [0$\bar{1}$1] directed single-crystal GaAs lines. Growth temperatures = 700°C, $AsH_3/TMG = 45$.

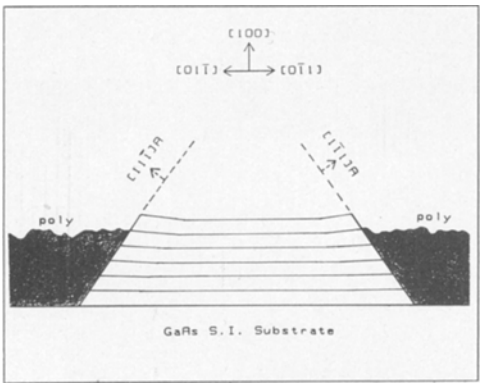

Fig. 8. Pictorial representation of typical [111]A and [111]A facets developing from the edge of [011] directed lines. The facets are 55° from the (100) S.I. GaAs surface.

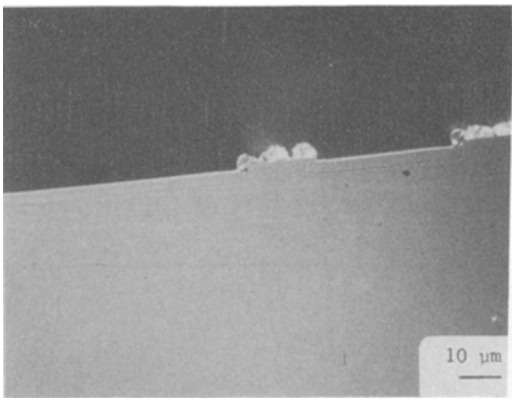

Fig. 10. Single-crystal GaAs growth in [011] directed troughs among homogeneous poly-GaAs. Flat surfaces and minimal sidewall growth are demonstrated within 1:1:10 ($NH_4OH:H_2O_2:H_2O$) etched trough. Growth temperature = 700°C, AsH_3/TMG = 45.

epitaxy at the interior of the single-crystal region, the growth is considered to be ordered two-dimensional growth on the (100) surface. However, at the very edge, the growth is forced to be three-dimensional and the epitaxy can proceed in all directions. If the growth is under mass transport, most of the Ga species which diffuse through the boundary layer will be incorporated into the crystal growth. Therefore the Ga constituents will migrate from the (111)A slow growth plane onto the (100) surface creating the (111)A facet at the edge. Even for selective growth at 700°C (P = 1 atm), which will produce a homogeneous poly/single-crystal interface, some pile-up at the boundary was observed. The inherent migration from the (111)A plane will generate growth rate increases at the interface. However, it is possible that at lower pressures, increased diffusion lengths will allow uniform enhancement across the entire single-crystal region eliminating edge pile-up (12). For [0$\bar{1}$1] directed lines of selective single crystal, the revealed {111} growth planes are 125° from the (100) surface and they protrude into the poly-GaAs region (Fig. 7b). The competition between the single-crystal material and the poly-GaAs at the interface will distort the {111} facets. Under this proposed scheme, it should be difficult to grow vertical junctions for (011) and (0$\bar{1}$1) directed lines at the mask/single-crystal interface independent of the mask material (between approximately 600° to 800°C). If the growth temperature is lowered into the kinetically controlled regime (around 600°C), the surface absorption should dominate the growth rate (25) and we have found that the (111)A slow growth plane can be eliminated (Fig. 9). Also, if the single-crystal lines are misoriented, then other facets will appear due to crystal orientation growth dependencies. However, the growth of other facets may have different growth mechanics and dependencies than the {111} facet since the atomic surface structure will be different (5). Although the mask material and/or growth pressure do not strongly affect the facet formation at the oxide/single-crystal interface, it will decide the extent of surface diffusion on all surfaces, thereby varying the amount of pile-up at the single-crystal edge. If the geometries of the single-crystal region are smaller than the diffusion length of the Ga-bearing species on the GaAs surface then the pile-up can be eliminated for masks that allow significant surface diffusion. Although the mask material and growth parameters are important elements in selective epitaxy, the crystal orientation and geometries are also crucial factors which can be chosen for specific device applications.

Filling isolated pockets.—To generate substrate isolated pockets of epitaxial materials, the openings of the oxide mask were etched 3-4 μm deep into the substrate prior to the growth. Now, the faceting and orientation of the etched sidewalls becomes imperative as the growth from the sidewall planes will interfere with the growth from the pocket bottom. A 1:1:10 ($NH_4OH:H_2O_2:H_2O$) etch gave nearly vertical walls traveling in the [011] direction. For a slightly less than or greater than 90° wall, growth from the walls caused a small defective region at the edge of the pocket. When a 90° wall was generated, growth on this face was minimal and the expected (111)A facet appeared at the edge of the pocket (Fig. 10-12). Lines etched in the [0$\bar{1}$1] direction with this etch were mesa shaped. Growth in these regions was parallel to both the flat bottom and the sloped sidewalls similar to those shown in Fig. 6b.

The 1:1:8 ($H_2SO_4:H_2O_2:H_2O$) solution was also used to etch patterns into the substrate. The sidewalls traveling

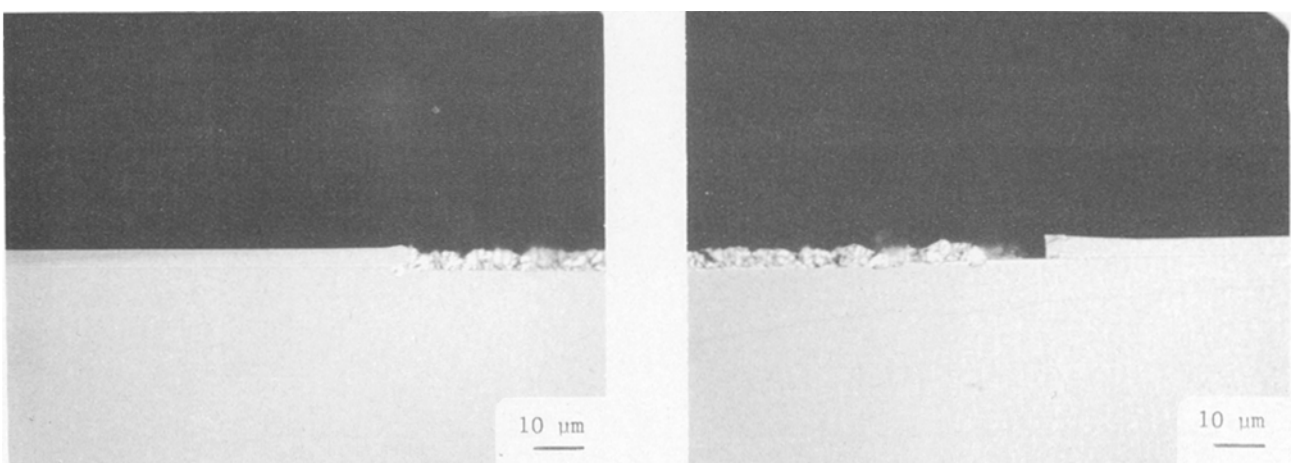

Fig. 9. Elimination of {111} facets for (a, left) [011] directed single-crystal lines and (b, right) [0$\bar{1}$1] directed single-crystal GaAs lines. The [0$\bar{1}$1] directed lines also reveal lateral overgrowth onto the native oxide mask. Growth temperature = 600°C, AsH_3/TMG = 45.

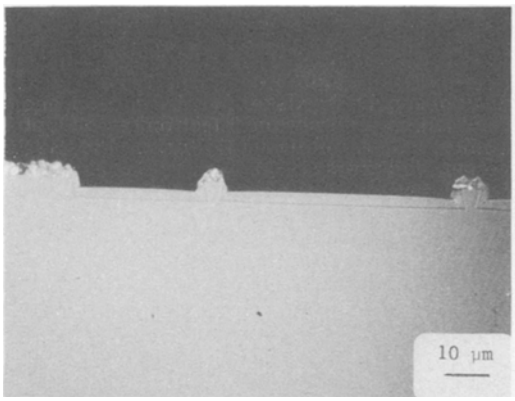

Fig. 11. A less vertical 1:1:10 ($NH_4OH:H_2O_2:H_2O$) etched wall exhibits more sidewall growth of the single-crystal GaAs within the [011] directed trough. Growth temperature = 700°C, AsH_3/TMG = 45.

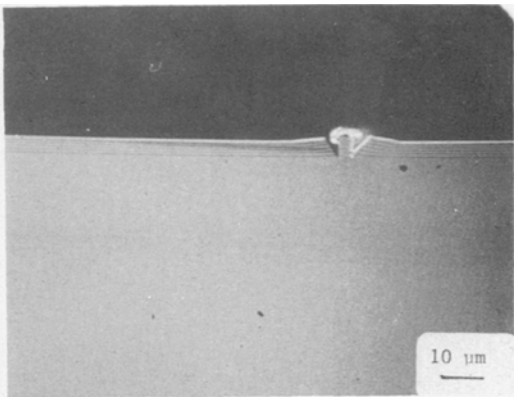

Fig. 12. Emergence of the [1$\bar{1}$1]A and [11$\bar{1}$]A facets from the bottom of a near vertical wall trough. Minimal growth occurs on the sidewall of the [011] directed trough. Growth temperature = 700°C , AsH_3/TMG = 45.

in the (011) direction have two facets and the resulting growth emerged from both of these side facets. The lack of nearly vertical sidewalls caused enhanced distortion of the growth at the pocket edges. Hence, less experiments were performed with this etch system since it does not render the more desirable vertical wall in the (011) direction.

Electrical and optical characterization.—Hall effect and photoluminescence (PL) measurements made on the 3 × 3 mm single-crystal patches indicated that the quality of the material was unaffected by the surrounding poly-GaAs and native oxide. For unintentionally doped single layers grown on unpatterned substrates, net carrier concentrations ranging from 3 to 6 × 10^{14} cm^{-3} and liquid nitrogen mobilities (μ_{77}) between 100 and 130 × 10^3 cm^2/Vs have been obtained. In the selective growth experiments, the 3 × 3 mm patches of undoped material exhibited mobilities from 100 to 105 × 10^3 cm^2/Vs, while the μ_{77} measured on an unpatterned control piece was 95,000 cm^2/Vs.

The polycrystalline GaAs deposited on the oxide mask was found to be highly resistive. The low field resistivities of 3 μm thick undoped, heavily-doped, or alternatively doped (marker layers), poly-GaAs layers were generally equivalent. The poly-GaAs electrical properties are similar to previously reported results (10) and the high defect densities at the grain boundaries are thought to be responsible for the high resistivity. These results indicate that large islands of high quality GaAs separated by semi-insulating poly GaAs can be obtained using native oxide masks.

Shown in Fig. 13 is a comparison of the PL spectra taken from a 3 × 3 mm selectively grown single-crystal patch and an unpatterned sample. The similarity of the two spectra re-emphasizes the high quality of the selectively grown GaAs. We, as well as other researchers, have found that undoped polycrystalline GaAs has extremely low relative luminescence efficiency (8, 25). Also AlGaAs/GaAs mutiple quantum wells (QW's) grown on an oxide patterned substrate have been investigated. Again, distinct and strong QW signals were detected at the 3 × 3 mm patches (26). Unlike the undoped single-layer poly-GaAs, the polycrystals of the QW (poly-QW's) exhibited much stronger photoluminescence. Compared with the single-crystal QW spectra, the full width at half maximum (FWHM) of the poly-QW's was significantly enlarged and the peak position shifted to the lower energy side of the spectrum. Further investigation of the poly-QW's is underway.

Summary

A selective area growth study by atmospheric pressure OMCVD using GaAs native oxide masks was conducted. GaAs semi-insulating substrates were oxidized in a plasma system and patterned by standard photolithography. Unpatterned wafers were typically placed adjacent to patterned ones during growth for comparison. Single crystal grown in mask windows has comparable high quality to those grown on the unpatterned substrates, as determined by their photoluminescent spectra and Hall mobilities. At the edges of the selectively grown areas, the facet formation is primarily dependent on the crystal orientation when the growth is conducted in the mass transport regime. Polycrystalline coverage on the oxide-masked regions was found to be affected by the growth temperature, V/III ratio, and mask geometry. The poly-GaAs has extremely high resistivity even though heavily doped, indicating its strong potential for isolation applications. Finally, the undoped poly-GaAs exhibits an extremely weak PL signal, but the polycrystalline quantum well structures have strong luminescence efficiency.

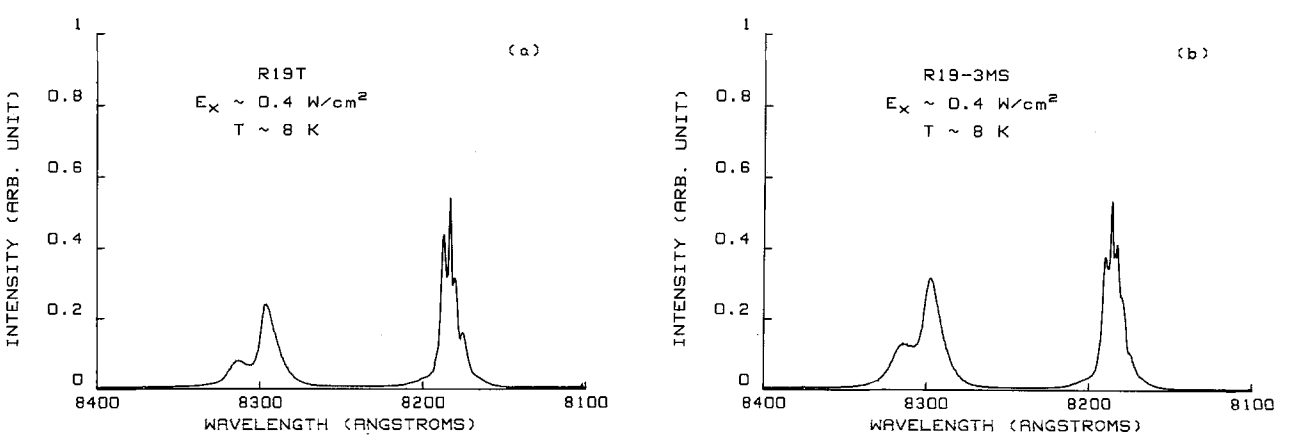

Fig. 13. Comparison of photoluminescence spectra of (a, left) unpatterned test wafer, (b, right) single-crystal region on an oxide patterned substrate.

Acknowledgments

This work was supported in part by the National Science Foundation under grant no. ECS-83073696. The authors would like to thank Mr. J. K. Hsu, Mr. D. C. Bertolet, and Mr. C. Musante for their technical assistance and many helpful discussions. Also, we would like to thank Mr. W. Sundburg and Gaetner Scientific for the ellipsometry data.

Manuscript submitted March 2, 1987; revised manuscript received June 8, 1987.

REFERENCES

1. D. W. Shaw, *This Journal*, **113,** 904 (1966).
2. G. D. Stareev and M. M. Piskorski, *Solid-State Electron.*, **20,** 161 (1977).
3. O. Ishihara, M. Otsubo, and S. Mitsui, *Jpn. J. Appl. Phys.*, **16,** 2109 (1977).
4. S. Iida and K. Ito, *J. Cryst. Growth*, **13-14,** 336 (1972).
5. H. Asai and S. Ando, *This Journal*, **132,** 2445 (1985).
6. R. P. Gale, R. W. McClelland, J. C. C. Fan, and C. O. Bozler, *Appl. Phys. Lett.*, **41,** 545 (1982).
7. Y. Takahashi, S. Sakai, and M. Umeno, *J. Cryst. Growth*, **68,** 206 (1984).
8. K. Nakai and M. Ozeki, *ibid.*, **68,** 200 (1984).
9. W. T. Tsang and M. Ilegems, *Appl. Phys. Lett.*, **31,** 301 (1977).
10. S. Hiyamizu, K. Nanbu, T. Fugii, T. Sakarai, H. Hashimoto, and O. Kyuzan, *This Journal*, **127,** 1562 (1980).
11. G. M. Metze, H. M. Levy, D. W. Woodward, C. E. C. Wood, and L. F. Eastman, *Appl. Phys. Lett.*, **37,** 628 (1980).
12. K. Kamon, S. Takagishi, and H. Mori, *J. Cryst. Growth*, **73,** 73 (1985).
13. Y. H. Lo, J. M. Hong, M. C. Wu, and S. Wang, *IEEE Electron Device Lett.*, **EDL-7,** 586 (1986).
14. A. H. Johnson, D. W. Kisker, W. M. Simpson, and R. D. Feldman, in "Picosecond Electronics and Optoelectronics," G. A. Mourou, Editor, p. 188, Springer-Verlag, New York (1985).
15. W. Margulis and W. Sibett, *Appl. Phys. Lett.*, **42,** 975 (1983).
16. R. P. H. Chang, D. L. Allara, and C. C. Chang, *J. Vac. Sci. Technol.*, **16**(3), 888 (1979).
17. T. Sugano and Y. Mori, *This Journal*, **121,** 113 (1974).
18. S. Iida and K. Ito, *ibid.*, **118,** 768 (1971).
19. R. P. Gale, R. W. McClelland, J. C. C. Fan, and C. O. Bozler, The Institute of Physics Conferences, **65** 101 (1983).
20. "Surface Mobilities on Solid Materials: Fundamental Concepts and Applications", T. B. Vu, Editor, NATO ASI Series, Plenum Press, New York (1981).
21. J. Nishizawa and T. Kurabayaski, *This Journal*, **130,** 413 (1983).
22. S. H. Hersee, E. Barbier, and R. Blondeau, *J. Cryst. Growth*, **77,** 310 (1986).
23. D. H. Reep, Ph.D. Thesis, Rensselaer Polytechnic Institute, Troy New York (1982).
24. J. B. Logan, M. Oberlin, L. Hollan, and R. Cadoret, *J. Cryst. Growth*, **19,** 176 (1975).
25. D. H. Reep and S. K. Ghandi, *This Journal*, **130,** 675 (1983).
26. K. M. Lau, S. H. Jones, J. K. Hsu, and D. C. Bertolet, in Proceedings of SPIE Advances in Semiconductors and Semiconductor Structures Conference, Bay Point, FL, **796,** 199 (1987).

In Situ Analyses of Photoexcitation Effects on $GaCl_3$

Jun-ichi Nishizawa,* Hidenori Shimawaki, and Yoshiki Sakuma

Research Institute of Electrical Communication, Tohoku University, Katahira, Sendai 980, Japan

ABSTRACT

Photoexcitation effects on $GaCl_3$ were investigated by means of infrared spectroscopy. By evaluating an emission band at 464 cm^{-1} corresponding to $GaCl_3$, it has been ascertained that $GaCl_3$ is excited in the vapor phase by irradiation with a 249 or 193 nm laser and the reaction with H_2 is promoted even at temperatures below 400°C, where the partial reduction of $GaCl_3$ by H_2 barely proceeds in the absence of irradiation. With nitrogen as a carrier gas, no change was observed in its emission intensity over the temperature range of 270° ~ 800°C in spite of irradiation with an excimer laser. Similar effects based on the photoexcitation of $GaCl_3$ were observed also in a GaAs-$AsCl_3$-H_2 system and proved to induce an enhancement of GaAs deposition in the presence of an arsenic source.

The preparation of defect-free crystals is quite important for the development of semiconductor devices. Especially in III-V compound semiconductors such as GaAs, nonstoichiometric defects, which are easily generated at high temperatures because of the high vapor pressures of the group V elements, are one of the most serious problems for the fabrication of reliable devices of high performance (1). Crystal growth under controlled arsenic vapor pressure is an effective method for obtaining stoichiometrically controlled GaAs crystals (2-5). It is no exaggeration to say that extended studies on the growth mechanism of Si and GaAs vapor-phase epitaxy (VPE) have thrown a new light on the investigation of chemical reaction processes. For instance, gas phase reactions in the chemical vapor deposition (CVD) of Si and GaAs were examined by means of infrared spectroscopy (6-8), Raman spectroscopy (9), and mass spectrometry (10). Moreover, molecular layer epitaxy (MLE) has made it possible to analyze the process of adsorption and surface reactions in the CVD of GaAs experimentally by mass spectrometry of desorption species (12). At the present time, there have been few reports of the theoretical estimation of the adsorbed species (13).

Recent attention has been directed to low temperature processes based on photoexcitation effects. In these processes, one can control elemental reaction steps individually and precisely by selecting the photon energy and intensity of the exciting light source. Not only was the growth rate in GaAs VPE enhanced (11-14), but the surface morphology and the crystalline quality of grown layers in Si VPE and in GaAs MLE were improved by irradiation using an ultraviolet (UV) light onto a substrate (15, 16). The latter is presumably caused by the enhancement of surface migration of adsorbed species. Such photoexcited processes relating to semiconductor fabrication were proposed by J. Nishizawa (17). In order to keep them under optimum control, it is necessary to identify the radicals and ions which contribute to a desired reaction, and to have a full knowledge of the wavelengths of the exciting source suitable for forming those species. The direct (*in situ*) observation of the gas in a reactor is indispensable to the understanding of the chemical reaction processes. As an example, this paper describes the results of a basic investigation into the photoexcitation effects on $GaCl_3$. It plays an important role in the halide VPE of GaAs. Previously, we reported on the reaction mechanism of GaAs halide VPE, where the significant photoinduced reactions were attributed to the photoexcitation of $GaCl_3$ (18). In the present work, *in situ* analyses have been performed in detail by means of infrared spectroscopy using direct observation.

*Electrochemical Society Active Member.